

Potent Peptide Inhibitors of Human Hepatitis C Virus NS3 Protease Are Obtained by Optimizing the Cleavage Products

Paolo Ingallinella, Sergio Altamura, Elisabetta Bianchi, Marina Taliani, Raffaele Ingenito, Riccardo Cortese, Raffaele De Francesco, Christian Steinkühler, and Antonello Pessi*

Istituto di Ricerche di Biologia Molecolare P. Angeletti (IRBM), Via Pontina Km 30.600, 00040 Rome, Italy

Received February 9, 1998; Revised Manuscript Received April 9, 1998

ABSTRACT: In the absence of a broadly effective cure for hepatitis caused by hepatitis C virus (HCV), much effort is currently devoted to the search for inhibitors of the virally encoded protease NS3. This chymotrypsin-like serine protease is required for the maturation of the viral polyprotein, cleaving it at the NS3–NS4A, NS4A–NS4B, NS4B–NS5A, and NS5A–NS5B sites. In the course of our studies on the substrate specificity of NS3, we found that the products of cleavage corresponding to the P6–P1 region of the substrates act as competitive inhibitors of the enzyme, with IC_{50} s ranging from 360 to 1 μ M. A detailed study of product inhibition by the natural NS3 substrates is described in the preceding paper [Steinkühler, C., et al. (1997) *Biochemistry* 37, 8899–8905]. Here we report the results of a study of the structure–activity relationship of the NS3 product inhibitors, which suggest that the mode of binding of the P region-derived products is similar to the ground-state binding of the corresponding substrates, with additional binding energy provided by the C-terminal carboxylate. Optimal binding requires a dual anchor: an “acid anchor” at the N terminus and a “P1 anchor” at the C-terminal part of the molecule. We have then optimized the sequence of the product inhibitors by using single mutations and combinatorial peptide libraries based on the most potent natural product, Ac-Asp-Glu-Met-Glu-Glu-Cys-OH ($K_i = 0.6 \mu$ M), derived from cleavage at the NS4A–NS4B junction. By sequentially optimizing positions P2, P4, P3, and P5, we obtained several nanomolar inhibitors of the enzyme. These compounds are useful both as a starting point for the development of peptidomimetic drugs and as structural probes for investigating the substrate binding site of NS3 by modeling, NMR, and crystallography.

Hepatitis C virus (HCV¹), a member of the Flaviviridae family, is the principal etiologic agent of both parenterally transmitted and sporadic non-A non-B hepatitis (1, 3). It is estimated that over 50 million people worldwide are infected by the virus (4); in more than half of these individuals, the infection becomes chronic, and liver cirrhosis develops in approximately 20% of the cases (5). Moreover, HCV is suspected to play a role in the onset of hepatocellular carcinoma (6). Neither an effective therapy for HCV-associated chronic hepatitis nor a vaccine for preventing HCV infection has to date been developed. A general strategy for the development of antiviral agents is inactivation of virally encoded proteases which are essential for replication (7). In the case of HCV, the generation of the mature

nonstructural portion of the HCV polyprotein, i.e., proteins NS2–NS3–NS4A–NS4B–NS5A–NS5B (arranged in this order), depends on the activity of two proteases. The first one, as yet poorly characterized, cleaves at the NS2–NS3 junction (8–10). The second one is a chymotrypsin-like serine protease contained within the N-terminal region (amino acids 1–180) of NS3 (henceforth NS3 protease). It accomplishes all the cleavages downstream of NS3, i.e., at the NS3–NS4A, NS4A–NS4B, NS4B–NS5A, and NS5A–NS5B junctions (11–16). It has been shown that the cleavage between NS3 and NS4 is intramolecular (cis), while all the remaining sites are processed in trans.

In vivo, NS3 is a heterodimer formed by the protease itself and the NS4A protein; the latter is a 54-residue protein which binds to the N-terminal region of NS3 via a central hydrophobic domain spanning residues 21–34 (17–22). NS4A enhances cleavage at all sites, and its presence is an absolute requirement for in vivo processing of the NS4B–NS5A junction (17). Several studies have shown that a peptide encompassing the central hydrophobic region of NS4A is sufficient as an activating cofactor for NS3 (21, 23–27).

Recently, two groups have independently reported the crystal structure of the recombinant protease, with (28) or without (29) the NS4A peptide cofactor; Koch and Bartsch-Schlager (30) using an intracellular trans cleavage assay and extensive mutagenesis of NS3 have further confirmed

* To whom correspondence should be addressed. Telephone: +39-6-91093445. Fax: +39-6-91093654. E-mail: pessi@irbm.it.

¹ Abbreviations: CHAPS, 3-(3-cholamidopropyl)dimethylammonio-1-propanesulfonate; DIEA, diisopropylethylamine; DMAP, *N,N'*-(dimethylamino)pyridine; DMF, *N,N'*-dimethylformamide; DMSO, dimethyl sulfoxide; DTT, dithiothreitol; Fmoc, 9-fluorenylmethyloxycarbonyl; HCV, (human) hepatitis C virus; HATU, *O*-(7-azabenzotriazol-1-yl)-1,1,3,3-tetramethyluronium hexafluorophosphate; HOBt, *N*-hydroxybenzotriazole; Pep4AK, amino acids 1678–1691 of the HCV polyprotein sequence encompassing the central hydrophobic domain of the NS4A protein sufficient for NS3 activation, with three additional non-HCV N-terminal lysine residues, sequence KKKGSVVIVGRILSGR-NH₂; PyBOP, (benzotriazol-1-yloxy)tris(pyrrolidino)phosphonium hexafluorophosphate; *t*-Bu, *tert*-butyl; TFA, trifluoroacetic acid; TNBS, trinitrobenzenesulfonic acid.

that the main determinant of substrate binding is phenylalanine 154, with an additional minor role for alanine 157.

Initially, the substrate specificity of NS3 has been qualitatively investigated using transient transfection (31, 32), in vitro translation (33), or intracellular processing of fusion proteins in *Escherichia coli* (34). More recently, efficient heterologous expression and purification of the enzymatically active protease domain have been described (24, 35–43), and optimized conditions for the determination of protease activity have been established (43–45). This has allowed a systematic study of NS3 substrate specificity using synthetic peptides derived from the NS4A–NS4B (46) or NS5A–NS5B cleavage sites (47, 48).

In the course of our studies on the substrate specificity of NS3, we found that one of the products of cleavage of the NS4A–NS4B peptide (Ac-DEMEEC-OH) acts as a competitive inhibitor of NS3 with a K_i of 0.6 μM (see ref 60). Although not unprecedented (49–52), this is unusual for serine proteases, and we sought confirmation by the synthesis of the corresponding product inhibitors derived from the NS5A–NS5B (Ac-EDVVCC-OH) and NS4B–NS5A (Ac-DCSTPC-OH) junctions; these peptides also display a competitive behavior with K_i values of 3.2 and 180 μM , respectively. A detailed study of product inhibition by the natural NS3 substrates is reported in ref 60.

Here we show that product inhibition can be exploited by single-mutant and combinatorial optimization to yield nanomolar inhibitors of NS3 protease.

MATERIALS AND METHODS

Peptide Synthesis. Protected amino acids were commercially available from Novabiochem (Läufelfingen, Germany), Bachem (Bubendorf, Germany), Neosystem (Strasbourg, France), or Synthetech (Albany, NY). Peptide synthesis was performed by Fmoc/t-Bu chemistry (53) on Novasyn TGA (peptide acids) or Novasyn TGR (peptide amides) resin. The first residue of the C-terminal acids was esterified to the resin in the presence of DMAP according to Atherton and Sheppard (53). Individual peptide sequences were assembled on a Millipore 9050 Plus synthesizer, using PyBOP/HOBt/DIEA (1:1:2) activation, a 5-fold molar excess of acylants over the resin amino groups, and a coupling time of 30 min to 1 h. Multiple peptide synthesis and the assembly of combinatorial libraries were performed on a Zinsser SMPS 350 synthesizer using PyBOP/HOBt/DIEA (1:1:2) activation, a 5-fold molar excess of acylants, and a coupling time of 20 min to 2 h as judged by the standard ninhydrin and TNBS color tests, essentially as described (54–56). The undefined or “mixed” positions were incorporated by coupling a mixture of activated amino acids, with the relative ratios suitably adjusted to compensate for the differences in reactivity; near equivalence of the incorporation was assessed by quantitative amino acid analysis. Using this method, we achieve a maximum deviation from equimolarity of $\pm 30\%$ (56). The peptides were cleaved with 88% TFA, 5% phenol, 2% triisopropylsilane, and 5% water (57). Crude peptides were purified by reversed-phase HPLC on a Nucleosyl C18 column (250 \times 21 mm, 100 Å, 7 μm) using $\text{H}_2\text{O}/0.1\%$ TFA and acetonitrile/0.1% TFA as eluents. Analytical HPLC was performed on an Ultrasphere C18 column (250 \times 4.6 mm, 80 Å, 5 μm , Beckman). Purified

($\geq 95\%$) peptides were characterized by mass spectrometry, ^1H NMR, and amino acid analysis.

Enzyme Preparation. The protease domain of the NS3 protein (amino acids 1–180, followed by the sequence ASKKKK) of the HCV J strain was prepared and purified as previously described in ref 60.

Protease Activity Assays. Concentrations of stock solutions of peptides, prepared in DMSO or in buffered aqueous solutions and kept at -80°C until they were used, were determined by quantitative amino acid analysis performed on HCl-hydrolyzed samples. The HPLC enzymatic assay was performed in 57 μL of 50 mM Hepes (pH 7.5), 1% CHAPS, 15% glycerol, and 10 mM DTT (buffer A). In the experiments at high ionic strength, buffer A was complemented with 150 mM NaCl (buffer B). As the protease cofactor, we used a peptide spanning the central hydrophobic core (residues 21–34) of the NS4A protein, with a three-lysine tag at the N terminus to increase the solubility (27) of Pep4AK (KKKGSVVIVGRIILSGR-NH₂). Pep4AK (16 μM) was preincubated for 10 min with 10–50 nM protease. Inhibitors were added to the preformed protease–Pep4AK complex, and the mixture was incubated for a further 10 min. Enzyme concentrations were always kept at least 5 times below the K_i value of the inhibitor. Reactions were then started by addition of 3 μL of the substrate peptide Ac-DEMEECASHLPYK(Ac)-NH₂ (scissile Cys–Ala bond in bold) to yield a final concentration of 10 μM in buffer A and 500 μM in buffer B. These concentrations correspond to the K_m values under the respective assay conditions. To accurately determine potencies in the low nanomolar range, the fluorescent substrate peptide Ac-DEMEECASHLPYE-(EDANS)-NH₂ was used which permitted lowering of enzyme concentrations to 150 pM. Incubation times were chosen to produce $<7\%$ substrate conversion. The reaction was stopped by addition of 40 μL of 1% TFA, and the extent of substrate cleavage was determined by HPLC analysis as described (60). Dual detection was used for both the absorbance at 220 nm and the fluorescence of the tyrosine residue ($\lambda_{\text{ex}} = 260$ nm, $\lambda_{\text{em}} = 305$ nm) or for the EDANS fluorophore ($\lambda_{\text{ex}} = 355$ nm, $\lambda_{\text{em}} = 495$ nm). Cleavage products were quantitated by integration of chromatograms with respect to appropriate standards. Kinetic parameters were calculated from nonlinear least-squares fit of initial rates as a function of substrate concentration with the help of Kaleidagraph software, assuming Michaelis–Menten kinetics. IC_{50} values were calculated by fitting a two-parameter logistic function (eq 1) to the data:

$$\% \text{ residual activity} = 100/[1 + ([I]/\text{IC}_{50})^s] \quad (1)$$

where $[I]$ is the inhibitor concentration and s is the slope factor of the curve.

K_i values were calculated by fitting a modified version of the Michaelis–Menten equation to the data (eq 2):

$$V = V_{\text{max}}S/[K_m[1 + ([I]/K_i)] + S] \quad (2)$$

For the Microplate protease assay, the J strain protease was stored until it was used at -80°C in 250 mM NaCl, phosphate buffer (pH 6.5), 50% glycerol, and 0.1% CHAPS; Pep4AK was stored at -80°C in DMSO, and the tritiated substrate Ac-DEMEECASHLPYK-[^3H -Ac]-NH₂ and the cor-

responding cold substrate Ac-DEMEECASHLPYK(Ac)-NH₂ were stored at -80°C in DMSO/DTT. The assay was run in Costar polypropylene 96-well plates. The composition of the reaction mixture was as follows (100 mL): 15% glycerol, 30 mM DTT, 50 mM Hepes (pH 7.5), 0.05% Triton X-100, 10 nM protease, 5 μM tritiated and cold substrate (300 000 cpm), and 15 μM Pep4AK. The test compound, dissolved in DMSO, was diluted to a final concentration of 10% DMSO in the assay buffer. Pep4AK was preincubated with the protease for 5 min before addition of the substrate mix. Under these conditions, the K_m of the substrate was $7 \pm 2 \mu\text{M}$. The plates were shaken for 30 min at room temperature, and then 100 μL of 20% Fractogel TSK-DEAE 650S (Merck) was added to capture unreacted substrate and the plate shaken for another 10 min. After the resin was allowed to settle by gravity, 30 μL of the reaction mixture was transferred in a 96-well plate (Picoplate, Packard) and admixed with 250 μL of scintillation cocktail (Microscint 40) and the radioactivity measured in a Packard Top Count β -counter.

RESULTS

General Features of the Structure–Activity Relationship of the Product Inhibitors

The general features of the structure–activity relationship (SAR) of the product inhibitors were found to be identical for the peptides derived from the cleavage of the natural NS3 sites (with potency in the micromolar range) and for the optimized inhibitors with nanomolar potency (*vide infra*). Therefore, in this section, we prefer to illustrate the SAR using data from both series of compounds, instead of following the chronological order of the experiments. Optimization of the parent inhibitors is described in the following section. We follow the nomenclature of Schechter and Berger (58) in designating the cleavage sites as P6–P5–P4–P3–P2–P1...P1'–P2'–P3'–P4', with the scissile bond between P1 and P1' and the C terminus of the substrate on the prime site. The inhibitory potencies of the compounds are expressed as IC₅₀ values, since kinetic experiments to determine the mechanism and calculate K_i were only performed on selected peptides. Under our experimental conditions, $K_i \approx 0.5\text{IC}_{50}$.

C-Terminal Carboxylate. The activity of the product inhibitors is crucially dependent upon the presence of a free carboxyl at the C terminus. Substitution with a carboxamide or reduction to the alcohol resulted in a >100-fold reduction in activity [compare Ac-Asp-Glu-Met-Glu-Glu-Cys-OH with Ac-Asp-Glu-Met-Glu-Glu-Cys-NH₂ and Ac-Asp-Glu-Met-Glu-Glu-Cys(ol), IC₅₀ = 1, 160, and 130 μM , respectively]. The same trend was later observed in the optimized peptides (data not shown).

P1 Residue Substitutions. The effect of the P1 residue was studied in the NS4A-derived and in the optimized series; in order of decreasing potency, we found P1 = Cys > Abu (2-aminobutyric acid) (compare Ac-Asp-Glu-Met-Glu-Glu-Cys-OH and Ac-Asp-Glu-Met-Glu-Glu-Abu-OH, IC₅₀ = 1 and 5.8 μM , respectively) > Val (compare Ac-Asp-Glu-Leu-Glu-Cha-Cys-OH and Ac-Asp-Glu-Leu-Glu-Cha-Val-OH, IC₅₀ = 0.12 and 4 μM) > Ser > Gly (compare Ac-Asp-Glu-Met-Glu-Glu-Cys-OH, Ac-Asp-Glu-Met-Glu-Glu-Ser-OH, and Ac-Asp-Glu-Met-Glu-Glu-Gly-OH, IC₅₀ = 1, 41,

Table 1: Importance of P6–P5 Acidic Residues in the Binding of Product Inhibitors

	peptide ^a	IC ₅₀ (μM) ^b
NS4A-Derived Inhibitors		
1	Ac-Asp-Glu-Met-Glu-Glu-Cys-OH	1
2	Ac-Glu-Met-Glu-Glu-Cys-OH	21
3	Ac-Met-Glu-Glu-Cys-OH	150
4	Suc-Glu-Met-Glu-Glu-Cys-OH	1.3
5	Suc-Met-Glu-Glu-Cys-OH	77
6	Glut-Met-Glu-Glu-Cys-OH	69
NS5A-Derived Inhibitors		
7	Ac-Glu-Asp-Val-Val-Abu-Cys-OH	2.8
8	Suc-Asp-Val-Val-Abu-Cys-OH	4.6
9	Glut-Asp-Val-Val-Abu-Cys-OH	5.5
10	Ac-Glu-Asp-Val-Val-Cys-Cys-OH	5.3
11	Ac-Asp-Glu-Val-Val-Cys-Cys-OH	2.1
Optimized Inhibitors		
12	Ac-Asp-Glu-Dif-Glu-Cha-Cys-OH	0.05
13	Ac-Glu-Dif-Glu-Cha-Cys-OH	1.4
14	Ac-Dif-Glu-Cha-Cys-OH	30
15	Ac-Asp-Glu-Dif-Ile-Cha-Cys-OH	0.06
16	Ac-Glu-Dif-Ile-Cha-Cys-OH	2.4
17	Ac-Dif-Ile-Cha-Cys-OH	100

^a Abbreviations: Abu, 2-aminobutyric acid; Cha, β -cyclohexylalanine; Dif, 3,3-diphenylalanine; Glut, glutaryl; Suc, succinyl. ^b Under our experimental conditions, $K_i \approx 0.5\text{IC}_{50}$ (see the text).

and 62 μM , respectively). The P1 residue must be in the L-configuration, as shown in the NS5A-derived (compare Ac-Glu-Asp-Val-Val-Abu-Cys-OH and Ac-Glu-Asp-Val-Val-Abu-D-Cys-OH, IC₅₀ = 2.8 and 194 μM) and in the optimized series (compare Ac-Asp-Glu-Dif-Glu-Cha-Cys-OH and Ac-Asp-Glu-Dif-Glu-Cha-D-Cys-OH, IC₅₀ = 0.05 and 3.4 μM). Surprisingly, however, Ac-Asp-Glu-Met-Glu-Glu-D-Cys-OH is only 4-fold less potent (IC₅₀ = 4 μM) than Ac-Asp-Glu-Met-Glu-Glu-Cys-OH (IC₅₀ = 1 μM).

P1 Deletion Analogues. The combined effect of eliminating the contributions of the P1 side chain and the C-terminal carboxylate could be examined only in the optimized analogues, which retained a sufficient level of inhibitory activity. As expected, deletion of the P1 residue yields a ≥ 700 -fold decrease in activity (compare Ac-Asp-Glu-Dif-Glu-Cha-Cys-OH and Ac-Asp-Glu-Dif-Glu-Cha-OH, IC₅₀ = 0.05 and 120 μM). A free carboxyl is a better C-terminal group than a carboxamide or an *N,N*-dimethylamide also in these shortened analogues, although the difference is now only 2-fold; this modest effect could be due to the basic nature of the electrostatic surface of NS3 in the S6–S1 region, which favors negatively charged ligands [compare Ac-Asp-Glu-Dif-Glu-Cha-OH, Ac-Asp-Glu-Dif-Glu-Cha-NH₂, and Ac-Asp-Glu-Dif-Glu-Cha-N(CH₃)₂, IC₅₀ = 120, 210, and 245 μM , respectively]. Moreover, although much less potent, these P6–P2 pentapeptides remain competitive inhibitors of the enzyme (data not shown).

P6 and P5 Residues. Deletion of the acid in P6 causes a significant (>10-fold) decrease in activity, while simultaneous deletion of both the P6 and the P5 acids gives a >100-fold decrease. We found this in both the product inhibitor directly derived from NS4A (compare entries 1–3 in Table 1) and the optimized peptides, where the effect is even more pronounced (compare entries 12–14 as well as entries 15–17, Table 1). However, in both the NS4A and NS5A series, the P6 aspartic acid may be substituted with a simple carboxylic acid like succinic acid, with loss of the acety-

Table 2: Noncoded Amino Acids Used in the Xxx and Ooo Positions

amino acid ^a	code	chirality
L- α -aminobutyric acid	Abu	L
2-aminoisobutyric acid	Aib	L
β -alanine	β Ala	L
γ -aminobutyric acid	γ Abu	L
6-aminohexanoic acid	Ahx	L
methionine DL-sulfoxide	M(O)	L
β -cyclohexyl-L-alanine	Cha	L+D
1-amino-1-cyclohexanecarboxylic acid	Acx	L
γ -carboxyglutamic acid	Gla	L
homophenylalanine	Hof	L
hydroxyproline	Hyp	L
norleucine	Nle	L+D
norvaline	Nva	L+D
ornithine	Orn	L
4-chlorophenylalanine	Fcl	L+D
4-nitrophenylalanine	Fno	L
phenylglycine	Phg	L
sarcosine	Sar	L
thioprolin	SPro	L
(3S,4S)-4-amino-3-hydroxy-5-cyclohexylpentanoic acid	Ach	
(3S,4S)-4-amino-3-hydroxy-5-phenylpentanoic acid	Ahp	
5-aminovaleric acid	Ava	L
8-aminooctanoic acid	Aoc	L
α -diaminopropionic acid	α DP	L
β -diaminopropionic acid	β DP	L
(3S,4S)-4-amino-3-hydroxy-6-methylheptanoic acid	Sta	
1,2,3,4-tetrahydroisoquinoline-3-L-carboxylic acid	Tic	L+D
3,3-diphenylalanine	Dif	L+D
3-pyridylalanine	Pyr	L+D
2-naphthylalanine	Nap	L+D
4-thiazolylalanine	Thz	L+D
4-fluorophenylalanine	Pff	L+D
4-carboxymethylpiperazine	Cmpi	L

^a Beyond the amino acids listed in the table, all the natural amino acids with the exception of Cys are included in both the L- and D-configuration. The total number of amino acids used is 81.

lamino moiety (compare entries 1 with 4 and entries 7 with 8, Table 1); the exact length of the side chain is not important, since C-terminal succinic and glutaric acid are equivalent (compare entries 8 with 9, Table 1). This is true also for the P5 position, since deletion of P6-Asp and substitution of P5-Glu with either succinic or glutaric acid yield equipotent analogues (compare entries 5 and 6, Table 1). In line with a permissive binding of an acidic pair in P6–P5, Asp-Glu and Glu-Asp are both allowed as P6–P5 residues (compare entries 10 and 11, Table 1).

Optimization of the Product Inhibitors

Combinatorial Peptide Library in Positions P2–P4. Ac-Asp-Glu-Met-Glu-Glu-Cys-OH was taken as a starting point to optimize positions P2–P4. A combinatorial library was prepared in the format Ac-Asp-Glu-Xxx-Glu-Ooo-Cys-OH, with Ooo and Xxx defined as in Houghten et al. (59): Ooo = a defined amino acid, one of a panel of 81 amino acids, and Xxx = a mixed position, anyone of the amino acids of the same panel (Table 2). Overall, the library was composed of 81 mixtures of 81 peptides each. The peptides were tested as crude products coming from cleavage in the microplate assay at a final concentration of 6 μ M (Figure 1). The most active mixtures were those where Ooo = Leu and Cha. We synthesized the corresponding single-mutant analogues retaining the parent residue (Met) in position P4: Ac-Asp-

Glu-Met-Glu-Leu-Cys-OH ($IC_{50} = 1.1 \mu$ M) and Ac-Asp-Glu-Met-Glu-Cha-Cys-OH ($IC_{50} = 0.3 \mu$ M). P2 = Cha was therefore selected for the decoding of the P4 position. A set of 81 single-substitution analogues was synthesized in the format Ac-Asp-Glu-Ooo-Glu-Cha-Cys-OH (Figure 2). Many peptides inhibited NS3 to a greater extent than the parent where P4 = Met, namely, where P4 = Tha, Phe, Val, Fcl, Tyr, Nle, Ile, Cha, Phg, Leu, and Dif. The peptides were purified by HPLC and characterized by mass and NMR spectroscopy, and their IC_{50} values were determined (Table 3). The mechanism of inhibition was determined for the two most potent compounds, Ac-Asp-Glu-Leu-Glu-Cha-Cys-OH and Ac-Asp-Glu-Dif-Glu-Cha-Cys-OH; they are both competitive inhibitors with a K_i of 96 and 40 nM, respectively. The kinetic analysis for the latter peptide is shown in Figure 3.

Optimization of Position P3. Mainly because of the high cost of the amino acid Dif, the peptide where P4 = Leu was chosen as a starting point to optimize the P3 position. Like for P4, we prepared an 81-amino acid analogue set (Table 2) with the general structure Ac-Asp-Glu-Leu-Ooo-Cha-Cys-OH. The peptides were tested at a final concentration of 1 μ M (Figure 4). Only two residues yielded a potency comparable with the P3 = Glu, i.e., P3 = Val and Ile. The peptides were purified by HPLC, characterized by mass and NMR spectroscopy, and retested to determine the IC_{50} ; Ac-Asp-Glu-Leu-Val-Cha-Cys-OH and Ac-Asp-Glu-Leu-Ile-Cha-Cys-OH have IC_{50} values of 79 and 60 nM, respectively. When the Glu \rightarrow Ile substitution was included in the peptide where P4 = Dif, Ac-Asp-Glu-Dif-Ile-Cha-Cys-OH, we obtained an IC_{50} of 63 nM (competitive, $K_i = 30$ nM).

Optimization of Position P5. Ac-Asp-Glu-Leu-Glu-Cha-Cys-OH was again taken as a starting point also to optimize the P5 position. We synthesized a series of analogues with the general structure Ac-Asp-Ooo-Leu-Glu-Cha-Cys-OH, Ooo being the usual panel of 81 amino acids. The peptides were tested as crude products coming from cleavage in the microplate assay at a final concentration of 2 μ M (Figure 5). The IC_{50} s of the most active compounds after HPLC purification are given in Table 4. The most notable L-amino acid substitutions are P5 = Tyr ($IC_{50} = 135$ nM), which is as active as the parent peptide, and P5 = Gla ($IC_{50} = 55$ nM). Moreover, we found that in this position, at variance with all the others, D-amino acids are well tolerated (Table 4, entries 2–5, 7, 10, and 12). When a P5 D-residue was coupled with the P3 Glu \rightarrow Ile substitution, we obtained a 3-fold increase in potency (Table 4, entry 13). Finally, when the chirality of the best P5 L-residue was inverted, we obtained the most potent hexapeptide so far, Ac-Asp-D-Gla-Leu-Ile-Cha-Cys-OH ($IC_{50} = 1.5$ nM; Table 4, entry 14).

Comparison of the Potency of the Inhibitors in Low and High Ionic Strength Buffers. Optimization of the product inhibitors was carried out using a low-ionic strength buffer (see Materials and Methods). Under these conditions, the binding affinity of the product inhibitors is maximized, consistent with the electrostatic stabilization observed for the enzyme–substrate complex. The peptides resulting from each step of optimization were also tested using a higher ionic strength, i.e., in the presence of 150 mM NaCl. The IC_{50} s under both conditions are shown in Table 5. As might be expected, the sensitivity to ionic strength decreases with hydrophilic to hydrophobic substitutions: P2 Glu \rightarrow Cha

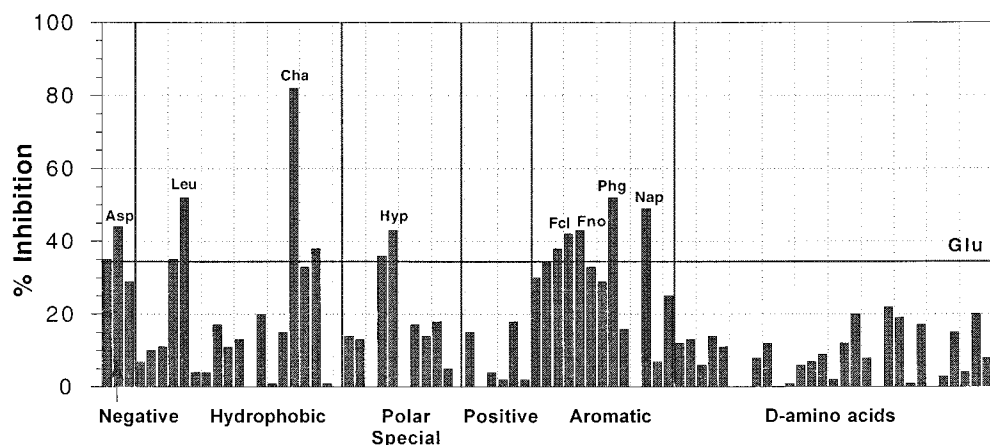


FIGURE 1: Optimization of position P2 of the product inhibitor Ac-Asp-Glu-Met-Glu-Glu-Cys-OH by screening of the 81 mixtures of the combinatorial library Ac-Asp-Glu-Xxx-Glu-Ooo-Cys-OH at a concentration of 6 μ M, using the microplate assay (see the text). The amino acids included in the Xxx and Ooo positions are shown in Table 2. For easier data readability, amino acids have been grouped according to their physicochemical properties: negative, Asp, Glu, and Gln; hydrophobic, Gly (reference), Val, Ile, Met, Leu, Ala, Abu, Aib, β Ala, γ Abu, Ahx, Ava, Aoc, M(O), Cha, Nle, Nva, and Sar; polar and/or special, Gln, Asn, Thr, Ser, Pro, Hyp, SPro, Sta, Ach, Ahp, and Cmpi; positive, Arg, Lys, His, Orn, α DP, β DP, and Pyr; aromatic, Trp, Tyr, Phe, Hof, Fcl, Fno, Pff, Phg, Tic, Dif, Nap, Thz, and Tha; and D-configuration, Val, Ile, Trp, Gln, Asn, Arg, His, Tyr, Pro, Phe, Met, Glu, Asp, Lys, Thr, Ser, Leu, Ala, Cha, Nle, Nva, Fcl, Phg, Tic, Dif, Pyr, Nap, Thz, and Pff. The classes of amino acids are separated by vertical lines, and a horizontal line is drawn at the height of the reference pool corresponding to the parent peptide, in this case P2 = Glu. For the most active pools, the identity of the amino acid is indicated above the corresponding bar.

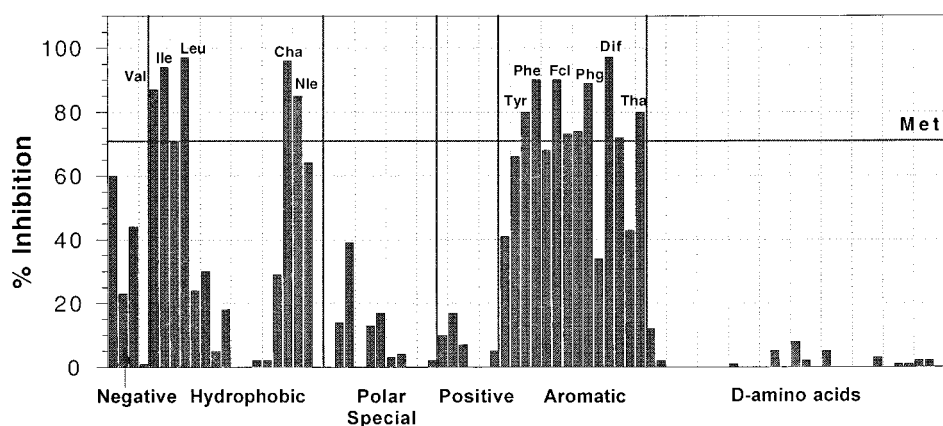


FIGURE 2: Optimization of position P4 of the product inhibitor Ac-Asp-Glu-Met-Glu-Glu-Cys-OH by screening of the 81-analogue set Ac-Asp-Glu-Ooo-Glu-Cha-Cys-OH. All the conditions are as described in the legend of Figure 1, except the concentration of the peptides, which was 2 μ M. The reference line is drawn at the height of P4 = Met.

Table 3: IC₅₀ Values for the P4 Analogues of Ac-Asp-Glu-Met-Glu-Cha-Cys-OH

	peptide ^a	IC ₅₀ (μ M)
1	Ac-Asp-Glu- Met -Glu-Cha-Cys-OH	0.350
2	Ac-Asp-Glu- Tha -Glu-Cha-Cys-OH	0.870
3	Ac-Asp-Glu- Phe -Glu-Cha-Cys-OH	0.420
4	Ac-Asp-Glu- Val -Glu-Cha-Cys-OH	0.330
5	Ac-Asp-Glu- Fcl -Glu-Cha-Cys-OH	0.300
6	Ac-Asp-Glu- Tyr -Glu-Cha-Cys-OH	0.236
7	Ac-Asp-Glu- Nle -Glu-Cha-Cys-OH	0.224
8	Ac-Asp-Glu- Cha -Glu-Cha-Cys-OH	0.140
9	Ac-Asp-Glu- Ile -Glu-Cha-Cys-OH	0.122
10	Ac-Asp-Glu- Phg -Glu-Cha-Cys-OH	0.120
11	Ac-Asp-Glu- Leu -Glu-Cha-Cys-OH	0.118
12	Ac-Asp-Glu- Dif -Glu-Cha-Cys-OH	0.055

^a Abbreviations like those used in Table 2.

(compare entries 1 and 3) and P3 Glu \rightarrow Ile (compare entries 4 and 5) but not P4 Met \rightarrow Dif (compare entries 3 and 4) and P5 Glu \rightarrow D-Glu (with P4 Dif \rightarrow Leu) (compare entries 5 and 6). When the three central amino acids are all hydrophobic, the sensitivity to the presence of salt is similar

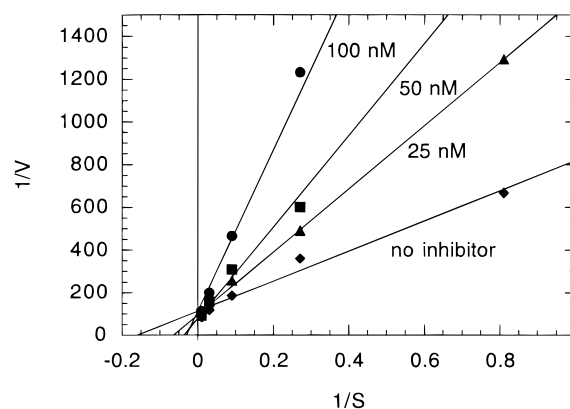


FIGURE 3: Lineweaver-Burk analysis of the optimized product inhibitor Ac-Asp-Glu-Dif-Glu-Cha-Cys-OH using 5 nM enzyme and inhibitor concentrations between 25 and 100 nM.

[P4-P2 = Val-Val-Cys (peptide entry 2), Dif-Ile-Cha (peptide entry 5), or Leu-Ile-Cha (peptide entry 6)], despite the significant difference in potency (IC₅₀ = 38 μ M, 50 nM, and 15 nM, respectively).

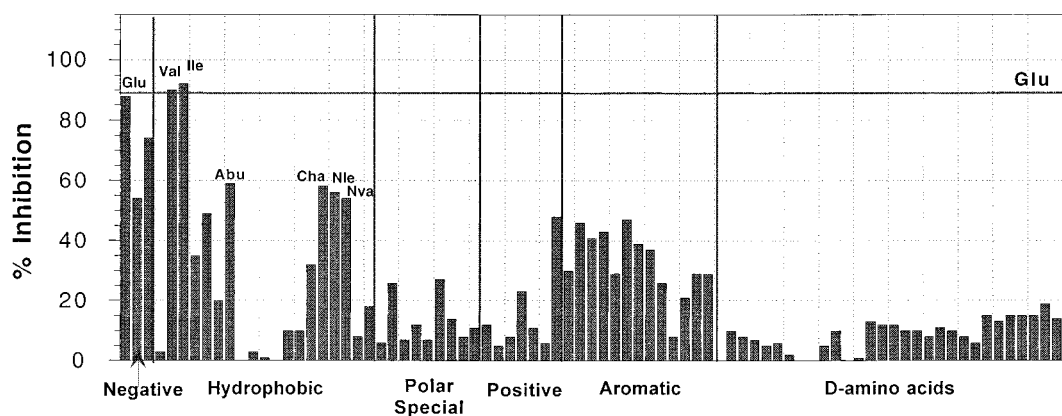


FIGURE 4: Optimization of position P3 of the product inhibitor Ac-Asp-Glu-Met-Glu-Glu-Cys-OH by screening of the 81-analogue set Ac-Asp-Glu-Leu-Ooo-Cha-Cys-OH. All the conditions are as described in the legend of Figure 1, except the concentration of the peptides, which was 1 μ M. The reference line is drawn at the height of P3 = Glu.

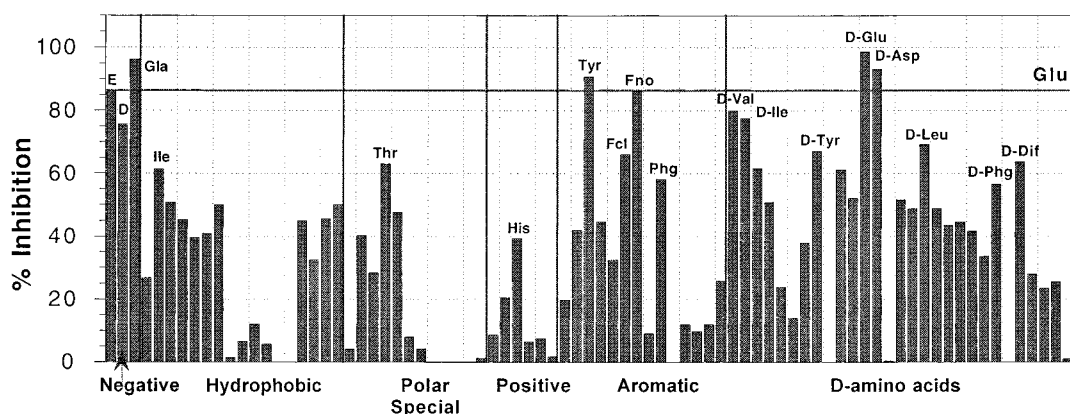


FIGURE 5: Optimization of position P5 of the product inhibitor Ac-Asp-Glu-Met-Glu-Glu-Cys-OH by screening of the 81-analogue set Ac-Asp-Ooo-Leu-Glu-Glu-Cha-Cys-OH. All the conditions are as described in the legend of Figure 1, except the concentration of the peptides, which was 2 μ M. The reference line is drawn at the height of P5 = Glu.

Table 4: IC₅₀ Values for the P5 Analogues of Ac-Asp-Glu-Leu-Glu-Cha-Cys-OH

	peptide ^a	IC ₅₀ (μ M)
1	Ac-Asp-Glu-Leu-Glu-Cha-Cys-OH	0.120
2	Ac-Asp-D-Phe-Leu-Glu-Cha-Cys-OH	0.820
3	Ac-Asp-D-Tyr-Leu-Glu-Cha-Cys-OH	0.680
4	Ac-Asp-D-Val-Leu-Glu-Cha-Cys-OH	0.470
5	Ac-Asp-D-Ile-Leu-Glu-Cha-Cys-OH	0.330
6	Ac-Asp-Asp-Leu-Glu-Cha-Cys-OH	0.290
7	Ac-Asp-D-Dif-Leu-Glu-Cha-Cys-OH	0.276
8	Ac-Asp-Fno-Leu-Glu-Cha-Cys-OH	0.240
9	Ac-Asp-Tyr-Leu-Glu-Cha-Cys-OH	0.135
10	Ac-Asp-D-Asp-Leu-Glu-Cha-Cys-OH	0.122
11	Ac-Asp-Gla-Leu-Glu-Cha-Cys-OH	0.055
12	Ac-Asp-D-Glu-Leu-Glu-Cha-Cys-OH	0.045
13	Ac-Asp-D-Glu-Leu-Ile-Cha-Cys-OH	0.015
14	Ac-Asp-D-Gla-Leu-Ile-Cha-Cys-OH	0.0015

^a Abbreviations like those used in Table 2.

DISCUSSION

The purpose of our work was to exploit the observation that NS3 is subject to significant product inhibition (60) to develop potent inhibitors of the enzyme. The starting point was therefore the sequence of the peptides derived from cleavage of the natural substrates. We first synthesized a series of analogues aimed at defining the general features of the SAR of the product inhibitors; these are illustrated in Figure 6.

The main contribution to the binding energy comes from the P1 amino acid, through both its side chain and its free

Table 5: IC₅₀ Values of Selected Product Inhibitors in the Absence and Presence of 150 mM NaCl

	peptide ^a	IC ₅₀ (μ M) ^b	IC ₅₀ (μ M) ^c with 150 mM NaCl
1	Ac-Asp-Glu-Met-Glu-Glu-Cys-OH	1.0	500
2	Ac-Glu-Asp-Val-Val-Cys-Cys-OH	5.3	38
3	Ac-Asp-Glu-Met-Glu-Cha-Cys-OH	0.35	13
4	Ac-Asp-Glu-Dif-Glu-Cha-Cys-OH	0.05	2
5	Ac-Asp-Glu-Dif-Ile-Cha-Cys-OH	0.06	0.8
6	Ac-Asp-D-Glu-Leu-Ile-Cha-Cys-OH	0.015	0.12
7	Ac-Asp-D-Gla-Leu-Ile-Cha-Cys-OH	0.0015	0.04

^a Abbreviations like those used in Table 2. ^b Experiments were performed using buffer A; see Materials and Methods. ^c Experiments were performed using buffer B; see Materials and Methods.

carboxylate (Table 3). The importance of a free carboxyl was highlighted by deletion with maintenance of the side chain, by substitution with a carboxamide, and by reduction to the corresponding alcohol; in all cases, we observed a >100-fold reduction in activity. The possible contacts between the enzyme and the C-terminal carboxylate have been discussed in ref 60. Not surprisingly, the side chain providing optimal occupancy of the S1 pocket of the enzyme is cysteine, followed in decreasing order of potency by 2-aminobutyric acid, valine, and serine; when P1 = Gly, the IC₅₀ increases 60-fold.

Even though the crucial role of the P1 residue has been underlined, it is however important to note that both the P1-deleted peptides and the C-terminally amidated hexapeptides

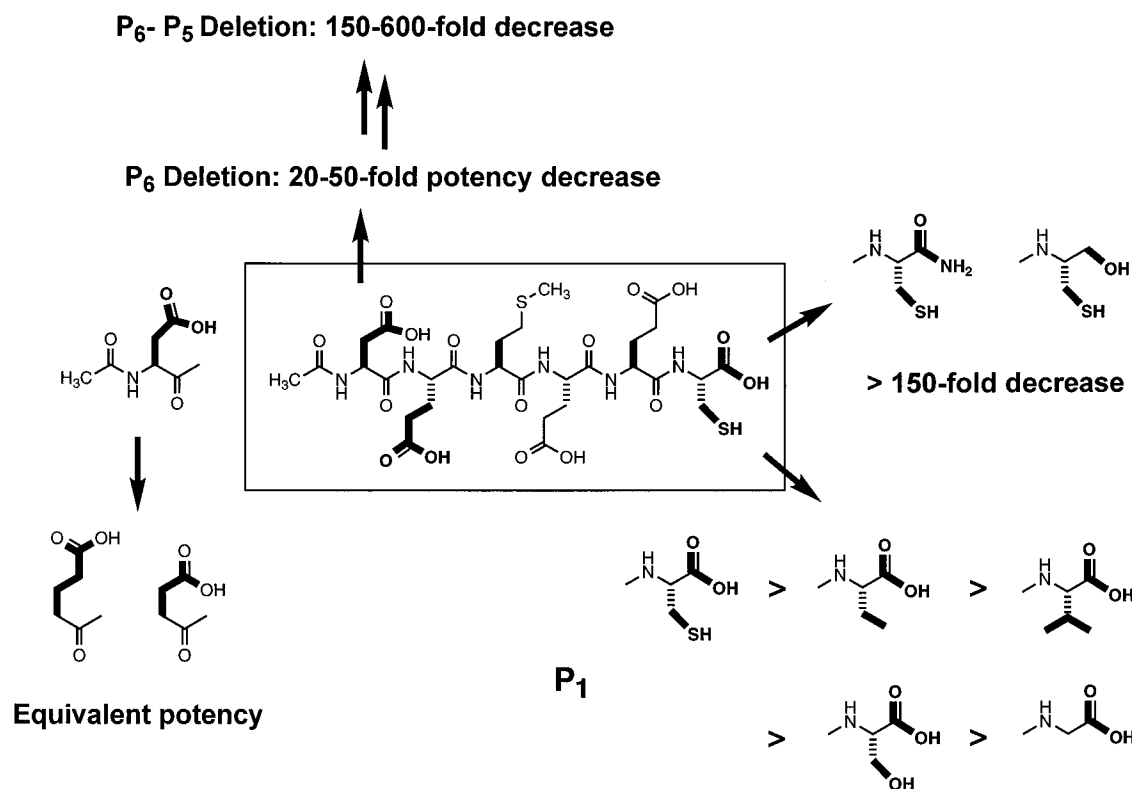


FIGURE 6: General features of the structure–activity relationship of the hexapeptide product inhibitors of hepatitis C virus NS3 protease. The features illustrated for peptide Ac-Asp-Glu-Met-Glu-Glu-Cys-OH ($K_i = 0.6 \mu\text{M}$) are valid for the inhibitors derived from all the natural cleavage sites and also for the nanomolar inhibitors obtained at the end of the optimization process (see the text).

are still competitive inhibitors of NS3. The complementary interaction of the P6–P5 acidic pair is as important as P1; their simultaneous deletion yields a >100-fold decrease in activity. Binding is rather permissive on the exact nature of the negatively charged moiety; achiral diacids with a C₄ or C₅ carbon chain are good substitutes for Asp in P6, and this is true also for the P5 position in the P5–P1 pentapeptides (Table 1).

We can now compare these general features of the SAR with the binding of the corresponding substrates. A detailed analysis of substrate specificity at the NS4A–NS4B (46) and NS5A–NS5B sites (47, 48) had shown that the main determinants of ground-state substrate binding to the enzyme (reflected in K_m) reside in the P6–P1 region. We have already discussed the contribution of the P1 residue. A negative charge in P6 is conserved in all cleavage sites. However, this preference is not very stringent since in the context of the decapeptide Ac-DEMEEECASHL mutation of Asp to Asn reduces ground-state affinity only 6-fold, and even inversion of the charge (Asp → Lys mutation) reduces K_m only 10-fold; notably, Asp → Ala mutation affects k_{cat} but not K_m values: $K_m = 105$ and $125 \mu\text{M}$, respectively. Alanine scanning of the same decapeptide had actually shown a greater reduction in K_m for the P5 rather than for the P6 acid (46). Zhang et al. (47) report very similar values of k_{cat}/K_m for alanine mutants in position P6 and P5 in the NS5A–NS5B substrate EDVVCCSMSYK (37 and $29 \text{ M}^{-1} \text{ s}^{-1}$, respectively). Finally, when using HCV polyprotein substrates, both P6 and P1 may undergo much more extensive mutagenesis with little effect on cleavage efficiency (31, 32). Our conclusion was that no single dominant factor explains the binding of NS3 substrates, which is mediated

by multiple interactions involving distal residues, notably, P6, P5, P1, and, to a lower extent, P3.

We have shown in ref 60 that the relative potency of the product inhibitors (NS4A > NS5A >> NS4B) correlates only partially to the K_m value of the uncleaved substrates, which is NS5A–NS5B > NS4A–NS4B >> NS4B–NS5A (43, 46). Our data nevertheless suggest that the mode of binding of the P region-derived product inhibitors is similar to the ground-state binding of the corresponding substrates, with additional binding energy provided by the C-terminal carboxylate. Optimal binding requires a dual anchor: an “acid anchor” at the N terminus and a “P1 anchor” at the C-terminal part of the molecule. Accordingly, Landro et al. (48) have recently described peptide inhibitors spanning the P6–P4′ region and found that they also extract most of their binding energy from the P side.

After we defined the general features of binding to NS3, our goal was to optimize the sequence of the product inhibitors. Toward this end, we decided to prepare combinatorial peptide libraries based on the NS4A-derived product, Ac-DEMEEC-OH, which was chosen by taking into account both the higher potency and the much better solubility. Our first combinatorial library was Ac-Asp-Glu-Xxx-Glu-Ooo-Cys-OH (Ooo = a defined position, and Xxx = a mixed position; see the Results). Screening of this library at a concentration of $6 \mu\text{M}$ showed that negatively charged and hydrophobic (both aliphatic and aromatic) residues are accepted in this position, while polar (Gln, Asn, Thr, and Ser), positively charged (Lys, Arg, His, αDP , and βDP), and conformationally constrained residues (Pro, SPro, and CmpI) are not accepted (with the partial exception of hydroxyproline). The chirality at P2 must be L, since all the D-amino

acid pools are inactive at this concentration (Figure 1). The best residue is β -cyclohexylalanine (Cha). The single-mutation analogue Ac-Asp-Glu-Met-Glu-Cha-Cys-OH was found to be 3-fold more active than the parent peptide ($IC_{50} = 0.3 \mu M$).

Therefore, we fixed Cha in position P2 and prepared the P4 analogue set Ac-Asp-Glu-Ooo-Glu-Cha-Cys-OH. It is apparent from Figure 2 and Table 3 that the P4 position has a strong preference for hydrophobic amino acids, both with aliphatic and with aromatic side chains, the best residue being 3,3-diphenylalanine (Dif), followed by leucine, isoleucine, and phenylglycine. Positively charged amino acids are detrimental to binding, a finding consistent with the previous studies on substrate specificity (46). Finally, the D-chirality is absolutely not tolerated; no D-amino acid is active in this position. Given the remarkable number of residues which scored better than the wild-type Met, some peptides were purified and retested (Table 3). The best combination for P4–P2 resulting from this optimization was therefore P4 = Dif and P2 = Cha. This peptide is fully competitive with NS3, with a K_i of 40 nM (Figure 3), an 18-fold improvement compared to that of the starting product inhibitor.

We then addressed position P3, with the analogue set Ac-Asp-Glu-Leu-Ooo-Cha-Cys-OH (instead of Dif, we used the less expensive amino acid Leu which is only 2-fold less active, Table 3). The results are very clear-cut (Figure 4); only two residues yielded a potency comparable with that for the case where P3 = Glu, i.e., P3 = Val and Ile. While other negatively charged and hydrophobic residues are tolerated (albeit less active), polar, conformationally constrained, positively charged, and D-amino acids are not accepted. It is notable that Glu and Val are the P3 residues in the two sequences corresponding to the best natural substrates and/or product inhibitors. The Glu \rightarrow Ile substitution in P3 yields Ac-Asp-Glu-Dif-Ile-Cha-Cys-OH, with a modest improvement in potency ($K_i = 30$ nM).

The optimized nanomolar inhibitors were used to confirm the general features of the SAR previously observed for the product inhibitors derived from the natural cleavage sites; we did not observe any qualitative or quantitative difference concerning the roles of the C-terminal carboxylate, the P1 side chain, and the P6–P5 acid pair (data not shown).

We finally examined position P5 in Ac-Asp-Ooo-Leu-Glu-Cha-Cys-OH (Glu was preferred in P3 to increase the solubility of the peptides). This analogue set gave the most unexpected results (Figure 5). First, a negative charge is not an absolute requirement in this position, since hydrophobic aromatic residues such as tyrosine and 4-nitrophenylalanine are equally good (Table 4). This is surprising since in the most potent natural product inhibitors we always find an acid in P5, while the hydrophobic amino acids found in the other products (Cys and Leu) score poorly in our library. Second, the D-chirality is well accepted in this position, with a range of activities going from 8-fold less active to 3-fold more active than L-Glu. This finding expands on the previous observation that the exact structure of the acid anchor moiety is permissive. A 3-fold increase in potency was obtained by coupling the inversion of chirality to the hydrophilic-to-hydrophobic P3 substitution Glu \rightarrow Ile: Ac-Asp-D-Glu-Leu-Ile-Cha-Cys-OH ($IC_{50} = 15$ nM; Table 4, entry 13). Finally, when we increased the negative charge density in P5 by substituting the dicarboxylic acid

D-Gla for D-Glu, we observed a further 10-fold increase in potency: Ac-Asp-D-Gla-Leu-Ile-Cha-Cys-OH with an IC_{50} of 1.5 nM (Table 4, entry 14).

We had previously shown that NS3 is susceptible to inhibition by increased ionic strength, with an about 50% drop in activity that can be detected by addition to the buffer of 50 mM NaCl. At 150 mM, the residual activity is only 20% (43). The effect of NaCl is to increase the K_m of the substrates and, according to what we have been observing so far, to increase the IC_{50} of the product inhibitors, presumably via destabilization of the P5–P6 interaction (Table 5). Because we observed this early in our study (60), the study of the SAR and the optimization of the product inhibitors were pursued in a buffer with low ionic strength. During the progress of the optimization, however, the peptides resulting from each incremental improvement in potency were also tested in high ionic strength (“high-salt” conditions), i.e., in the presence of 150 mM NaCl; the IC_{50} s under both conditions are shown in Table 5. We were pleased to observe that the increase in potency throughout the series was larger when considering the high-ionic strength data than when considering the low-ionic strength conditions. Overall, depending on the comparison used, the gain in inhibitory potency was between 600- and 10000-fold.

In conclusion, a detailed analysis of the structure–activity relationship of the peptide inhibitors derived from HCV protease substrates has enabled us to obtain much more potent compounds, which will be useful both as a starting point for the development of peptidomimetic drugs and as structural probes for investigating the binding site of NS3 by modeling, NMR, and crystallography. These studies are already in progress (D. Cicero et al., manuscript in preparation).

ACKNOWLEDGMENT

We thank Stefano Acali for help with the peptide synthesis, Francesca Naimo and Fabio Bonelli for mass spectrometry, Silvia Pesci for analytical NMR, Sergio Serafini, Nadia Gennari, Mauro Cerretani, Gabriella Biasiol, and Mirko Brunetti for the protease assays, Kristine Prendergast and Uwe Koch for computer modeling, and Victor G. Matassa for useful discussions and critical reading of the manuscript.

REFERENCES

1. Choo, Q. L., Kuo, G., Weiner, A. J., Overby, L. R., Bradley, D. W., and Houghton, M. (1989) *Science* 244, 359–362.
2. Kuo, G., Choo, Q. L., Alter, H. J., Gitnick, G. L., Redecker, A. G., Purcell, R. H., Myamura, T., Dienstag, J. L., Alter, M. J., Syevens, C. E., Tagtmeyer, G. E., Bonino, F., Colombo, M., Lee, W. S., Kuo, C., Berger, K., Shister, J. R., Overby, L. R., Bradley, D. W., and Houghton, M. (1989) *Science* 244, 362–364.
3. Houghton, M. (1996) in *Fields virology* (Fields, B. N., Knipe, D. M., and Howley, P. M., Eds.) 3rd ed., pp 1035–1058, Raven Press, New York.
4. Alter, H. J. (1995) *Blood* 85, 1681–1695.
5. Mast, E. E., and Alter, M. J. (1993) *Semin. Virol.* 4, 273–283.
6. Bisceglie, A. M. (1995) *Semin. Liver Dis.* 15, 64–69.
7. Krausslich, H. G., Oroszlan, S., and Wimmer, E. (1989) in *Viral Proteinases as Targets for Chemotherapy*, Vol. 57, Cold Spring Harbor Laboratory Press, Cold Spring Harbor, NY.

8. Hijikata, M., Mizushima, H., Akagi, T., Mori, S., Kakiuchi, N., Kato, N., Tanaka, T., Kimura, K., and Shimotohno, K. (1993) *J. Virol.* 67, 4665–4675.
9. Grakoui, A., McCourt, D. W., Wychowski, C., Feinstone, S., and Rice, C. M. (1993) *Proc. Natl. Acad. Sci. U.S.A.* 90, 10583–10587.
10. Pieroni, L., Santolini, E., Fipaldini, C., Pacini, L., Migliaccio, G., and La Monica, N. (1997) *J. Virol.* 71, 6373–6380.
11. Tomei, L., Failla, C., Santolini, E., De Francesco, R., and LaMonica, N. (1993) *J. Virol.* 67, 4017–4026.
12. Grakoui, A., McCourt, D. W., Wychowski, C., Feinstone, S. M., and Rice, C. M. (1993) *J. Virol.* 67, 2832–2843.
13. Bartenschlager, R. L., Ahlborn-Laake, L., Mous, J., and Jacobsen, H. (1993) *J. Virol.* 67, 3835–3844.
14. Eckart, M. R., Selby, M., Masiarz, F., Lee, C., Berger, K., Crawford, K., Kuo, C., Kuo, G., Houghton, M., and Choo, Q. L. (1993) *Biochem. Biophys. Res. Commun.* 192, 399–406.
15. Hijikata, M., Mizushima, H., Tanji, Y., Komoda, Y., Hirowatari, Y., Akagi, T., Kato, N., Kimura, K., and Shimotohno, K. (1993) *Proc. Natl. Acad. Sci. U.S.A.* 90, 10773–10777.
16. Komoda, Y., Hijikata, M., Tanji, Y., Hirowatari, Y., Mizushima, H., Kimura, K., and Shimotohno, K. (1994) *Gene* 145, 221–226.
17. Failla, C., Tomei, L., and De Francesco, R. (1994) *J. Virol.* 68, 3753–3760.
18. Lin, C., Pragai, B. M., Grakoui, A., Xu, J., and Rice, C. M. (1994) *J. Virol.* 68, 8147–8157.
19. Failla, C., Tomei, L., and De Francesco, R. (1995) *J. Virol.* 69, 1769–1777.
20. Tanji, Y., Hijikata, M., Satoh, S., Kaneko, T., and Shimotohno, K. (1995) *J. Virol.* 69, 4255–4260.
21. Lin, C., Thomson, J. A., and Rice, C. M. (1995) *J. Virol.* 69, 4273–4380.
22. Bartenschlager, R., Lohmann, V., Wilkinson, T., and Koch, J. A. (1995) *J. Virol.* 69, 7519–7528.
23. Tomei, L., Failla, C., Vitale, R. L., Bianchi, E., and De Francesco, R. (1996) *J. Gen. Virol.* 77, 1065–1070.
24. Shimizu, Y., Yamaji, K., Masuho, Y., Yokota, T., Inoue, H., Sudo, S., and Shimotohno, K. (1996) *J. Virol.* 70, 127–132.
25. Koch, J. O., Lohman, V., Herian, U., and Bartenschlager, R. (1996) *Virology* 221, 54–66.
26. Butkiewicz, N. J., Wendel, M., Zhang, R., Jubin, R., Pichardo, J., Smith, E. B., Hart, A. M., Ingram, R., Durkin, J., Mui, P. W., Murray, M. G., Ramanathan, L., and Daamapaptra, B. (1996) *Virology* 225, 328–338.
27. Bianchi, E., Urbani, A., Biasol, G., Brunetti, M., Pessi, A., De Francesco, R., and Steinkühler, C. (1997) *Biochemistry* 36, 7890–7897.
28. Kim, J. L., Morgenstern, K. A., Lin, C., Fox, T., Dwyer, M. D., Landro, J. A., Chambers, S. P., Markland, W., Lepre, C. A., O'Malley, E. T., Harbeson, S. L., Rice, C. M., Murcko, M. A., Caron, P. R., and Thomson, J. A. (1996) *Cell* 87, 343–355.
29. Love, R. A., Parge, H. E., Wickersham, J. A., Hostomsky, Z., Habuka, N., Moomaw, E. W., Adachi, T., and Hostomska, Z. (1996) *Cell* 87, 331–342.
30. Koch, J. O., and Bartenschlager, R. (1997) *Virology* 237, 78–88.
31. Kolykhalov, A. A., Agapov, E., and Rice, C. (1994) *J. Virol.* 68, 7525–7533.
32. Bartenschlager, R., Ahlborn-Laake, L., Yasargil, K., Mous, J., and Jacobsen, H. (1995) *J. Virol.* 69, 198–205.
33. Leinbach, S., Bhat, R., Xia, S. M., Hum, W. T., Stauffer, B., Davis, A., Hung, P. P., and Mizutani, S. (1994) *Virology* 204, 163–169.
34. Komoda, Y., Hijikata, M., Sato, S., Asabe, S. I., Kimura, K., and Shimotohno, K. (1994) *J. Virol.* 68, 7351–7357.
35. Kakiuchi, N., Hijikata, M., Komoda, Y., Tanji, Y., Hirowatari, Y., and Shimotohno, K. (1995) *Biochem. Biophys. Res. Commun.* 210, 1059–1065.
36. Overton, H., McMillan, D., Gillespie, F., and Mills, J. (1995) *J. Gen. Virol.* 76, 3009–3019.
37. D'Souza, E. D. A., Grace, K., Sangar, D. V., Rowlands, D. J., and Clarke, B. E. (1995) *J. Gen. Virol.* 76, 1729–1739.
38. Suzuki, T., Sato, M., Cjieda, S., Shoji, I., Harada, T., Yamakawa, Y., Watabe, S., Matsuura, Y., and Miyamura, T. (1995) *J. Gen. Virol.* 76, 3021–3029.
39. Steinkühler, C., Tomei, L., and De Francesco, R. (1996) *J. Biol. Chem.* 271, 6367–6373.
40. Shoji, I., Suzuki, T., Chieda, S., Sato, M., Harada, T., Yamakawa, Y., Watabe, S., Matsuura, Y., and Miyamura, T. (1996) *Hepatology* 22, 1648–1655.
41. Mori, A., Yamada, K., Kimura, J., Koide, T., Yuasa, S., Yamada, E., and Miyamura, T. (1996) *FEBS Lett.* 378, 37–42.
42. Hong, Z., Ferrari, E., Wright-Minogue, J., Chase, R., Risano, C., Seelig, G., Lee, C., and Kwong, A. D. (1996) *Anal. Biochem.* 240, 60–67.
43. Steinkühler, C., Urbani, A., Tomei, L., Biasol, G., Sardana, M., Bianchi, E., Pessi, A., and De Francesco, R. (1996) *J. Virol.* 70, 6694–6700.
44. Bianchi, E., Steinkühler, C., Taliani, M., Urbani, A., De Francesco, R., and Pessi, A. (1996) *Anal. Biochem.* 237, 239–244.
45. Taliani, M., Bianchi, E., Narjes, F., Fossatelli, M., Urbani, A., Steinkühler, C., De Francesco, R., and Pessi, A. (1996) *Anal. Biochem.* 240, 60–67.
46. Urbani, A., Bianchi, E., Narjes, F., Tramontano, A., De Francesco, R., Steinkühler, C., and Pessi, A. (1997) *J. Biol. Chem.* 272, 9204–9209.
47. Zhang, R., Durkin, J., Windsor, W. T., McNemar, C., Ramanathan, L., and Le, H. V. (1997) *J. Virol.* 71, 6208–6213.
48. Landro, J. A., Raybuck, S. A., Luong, Y. P. C., O'Maley, E. T., Harbeson, S. L., Morgenstern, K. A., Rao, G., and Livingston, D. J. (1997) *Biochemistry* 36, 9340–9348.
49. James, M. N. G., Sielecki, A. R., Brayer, G. D., and Delbaere, L. T. J. (1980) *J. Mol. Biol.* 144, 43–88.
50. Martin, P. D., Robertson, W., Turk, D., Huber, R., Bode, W., and Edwards, B. F. P. (1992) *J. Biol. Chem.* 267, 7911–7920.
51. Nienaber, V. L., Breddam, K., and Birkof, J. J. (1993) *Biochemistry* 32, 11469–11475.
52. Nienaber, V. L., Mersinger, L. J., and Kettner, C. A. (1996) *Biochemistry* 35, 9690–9699.
53. Atherton, E., and Sheppard, R. C. (1989) *Solid-phase peptide synthesis, a practical approach*, IRL Press, Oxford, U.K.
54. Wallace, A., Altamura, S., Toniatti, C., Vitelli, A., Bianchi, E., Delmastro, P., Ciliberto, G., and Pessi, A. (1994) *J. Pept. Res.* 7, 27–31.
55. Bianchi, E., Folgori, A., Wallace, A., Nicotra, M., Acali, S., Phalipon, A., Barbato, G., Bazzo, R., Cortese, R., Felici, F., and Pessi, A. (1995) *J. Mol. Biol.* 247, 154–160.
56. Wallace, A., Koblan, K. S., Hamilton, K., Marquis-Omer, D. J., Miller, P., Mosser, S. D., Omer, C. A., Schaber, M. D., Cortese, R., Oliff, A., Gibbs, J. B., and Pessi, A. (1996) *J. Biol. Chem.* 271, 31306–31311.
57. Sole, N. A., and Barany, G. (1992) *J. Org. Chem.* 57, 5399–5403.
58. Schechter, I., and Berger, A. (1967) *Biochem. Biophys. Res. Commun.* 27, 157–162.
59. Houghten, R. A., Pinilla, C., Blondelle, S. E., Appel, J. R., Dooley, C. T., and Cuervo, J. H. (1991) *Nature* 354, 84–86.
60. Steinkühler, C., Biasol, G., Brunetti, M., Urbani, A., Koch, U., Cortese, R., Pessi, A., and De Francesco, R. (1998) *Biochemistry* 37, 8899–8905.